Microbial community structure and sulfur biogeochemistry in mildly acidic sulfidic geothermal springs in Yellowstone National Park

Authors: Richard E. Macur, Zackary J. Jay, W.P. Taylor, M.A. Kozubal, B.D. Kocar, W.P. Inskeep

Microbial community structure and sulfur biogeochemistry in mildly-acidic sulfidic geothermal springs in Yellowstone National Park

R.E. MACUR,[1,2] Z.J. JAY,[1] W.P. TAYLOR,[1] M.A. KOZUBAL,[1] B.D. KOCAR[3] AND W.P. INSKEEP[1]

[1]*Thermal Biology Institute and Department of Land Resources and Environmental Sciences, Montana State University, Bozeman, MT, USA*
[2]*Center for Biofilm Engineering, Montana State University, Bozeman, MT, USA*
[3]*Stanford Synchrotron Radiation Lightsource, Menlo Park, CA, USA*

ABSTRACT

Geothermal and hydrothermal waters often contain high concentrations of dissolved sulfide, which reacts with oxygen (abiotically or biotically) to yield elemental sulfur and other sulfur species that may support microbial metabolism. The primary goal of this study was to elucidate predominant biogeochemical processes important in sulfur biogeochemistry by identifying predominant sulfur species and describing microbial community structure within high-temperature, hypoxic, sulfur sediments ranging in pH from 4.2 to 6.1. Detailed analysis of aqueous species and solid phases present in hypoxic sulfur sediments revealed unique habitats containing high concentrations of dissolved sulfide, thiosulfate, and arsenite, as well as rhombohedral and spherical elemental sulfur and/or sulfide phases such as orpiment, stibnite, and pyrite, as well as alunite and quartz. Results from 16S rRNA gene sequencing show that these sediments are dominated by Crenarchaeota of the orders Desulfurococcales and Thermoproteales. Numerous cultivated representatives of these lineages, as well as the Thermoproteales strain (WP30) isolated in this study, require complex sources of carbon and respire elemental sulfur. We describe a new archaeal isolate (strain WP30) belonging to the order Thermoproteales (phylum Crenarchaeota, 98% identity to *Pyrobaculum/Thermoproteus* spp. 16S rRNA genes), which was obtained from sulfur sediments using in situ geochemical composition to design cultivation medium. This isolate produces sulfide during growth, which further promotes the formation of sulfide phases including orpiment, stibnite, or pyrite, depending on solution conditions. Geochemical, molecular, and physiological data were integrated to suggest primary factors controlling microbial community structure and function in high-temperature sulfur sediments.

INTRODUCTION

Reduced species of sulfur (e.g., sulfide, elemental sulfur, and thiosulfate) are prevalent in geothermal habitats, and numerous hyperthermophiles have been shown to utilize various sulfur species as either electron donors or acceptors (Amend & Shock, 2001; Kletzin *et al.*, 2004; Huber & Stetter, 2006; Huber *et al.*, 2006; Ghosh & Dam, 2009). In fact, the term 'sulfur-dependent archaea' was originally used to describe the phylum Crenarchaeota until more recently when some isolates were shown to utilize other donors such as Fe(II) and H_2. Yellowstone National Park (YNP) contains a significant number of geothermal waters with high (e.g., > 10 μM) concentrations of dissolved sulfide (e.g., Allen & Day, 1935; McCleskey *et al.*, 2005). The equilibration of sulfidic waters with atmospheric oxygen results in the production of a variety of oxidized sulfur species, including elemental sulfur (S^0), thiosulfate, tetrathionate, polythionates, and sulfate (Xu *et al.*, 1998, 2000). In addition, reactions of sulfide with arsenic and other dissolved constituents may result in the production of complexes such as thioarsenates or thioarsenites,

depending on the concentration of oxygen and pH (Planer-Friedrich *et al.*, 2007, 2009; Helz & Tossell, 2008). Consequently, the multitude of possible abiotic and biotic reactions with sulfur species, as well as their potential transient nature, has made it difficult to understand the role of micro-organisms in high-temperature sulfidic sediments.

A number of studies have emphasized the importance of linking observed and predicted geochemical and microbial processes to develop a comprehensive understanding of the microbial ecology of geothermal systems (e.g., Reysenbach & Shock, 2002; Amend *et al.*, 2003; Macur *et al.*, 2004; Inskeep *et al.*, 2005; Meyer-Dombard *et al.*, 2005; Spear *et al.*, 2005; Rogers & Amend, 2006). Free-energy values of various oxidation–reduction reactions combined with the known physiologies of cultivated relatives have been used to infer the function of organisms identified using 16S rRNA sequence analysis (Macur *et al.*, 2004; Inskeep *et al.*, 2005; Spear *et al.*, 2005). For example, the highly exergonic oxidation of dissolved hydrogen using dissolved oxygen as an electron acceptor (knallgas reaction) coupled with the observation of numerous Aquificales-like 16S rRNA gene sequences has led scientists to implicate hydrogen as an important chemical energy source for microbial communities in various geothermal systems (Meyer-Dombard *et al.*, 2005; Spear *et al.*, 2005). Other studies suggest that oxidation–reduction reactions with reduced sulfur, ferrous–Fe, and/or nitrogen species may also serve as the basis for chemotrophic metabolism in extreme environments (Amend *et al.*, 2003; Rogers & Amend, 2005, 2006; D'Imperio *et al.*, 2008). Given the large number of thermodynamically favorable reactions involving the oxidation of reduced species in geothermal or hydrothermal waters (Amend & Shock, 2001; Inskeep *et al.*, 2005), more direct information regarding the mineralogy, aqueous geochemistry, and microbial community composition may provide clues on the processes important in sulfur cycling in geothermal environments.

The orders Sulfolobales, Thermoproteales, and Desulfurococcales (phylum Crenarchaeota) include isolates that utilize various forms of sulfur over a pH range of 2–8 (e.g., Zillig *et al.*, 1983; Segerer *et al.*, 1986; Itoh *et al.*, 2002; Prokofeva *et al.*, 2005; Boyd *et al.*, 2007). However, the role of various crenarchaea in mediating sulfur transformations in geothermal environments of YNP has not been studied extensively, and no representatives of the order Thermoproteales have been isolated from these extreme habitats. Consequently, the overall goal of this study was to develop a foundational understanding of the potential linkages between geochemical processes and microbial community structure in commonly observed high-temperature sulfur sediments in YNP. More specifically, the objectives of this work were to: (i) identify aqueous- and solid-phase geochemical processes occurring within high-temperature sulfur sediments ranging in pH from 4.2 to 6.1, (ii) determine the microbial community structure of hypoxic sulfur sediments using 16S rRNA gene sequencing, and (iii) characterize a relevant Thermoproteales isolated from sulfur sediments using in situ geochemical composition to design an appropriate cultivation medium. Geochemical, molecular, and physiological data were utilized together as a framework for understanding potential factors controlling microbial community structure and function in these high-temperature geothermal systems.

MATERIALS AND METHODS

Geothermal sites

Three sulfidic geothermal springs in YNP were selected to study relationships among aqueous- and solid-phase geochemistry, and microbial community composition and function over a pH range from ~4–6. One of the subject springs, unofficially referred to here as Joseph's Coat Spring 3 [JC3; UTMs (Easting/Northing = 553481/4954197; YNP Thermal Inventory Number JCS083], is located in the Joseph's Coat Springs complex ~13 km east of Canyon Village (YNP). The source pool of JC3 (3–4 m diameter, ~2 m deep) spouts continuously at 90 °C with a near-neutral pH of ~6.1 (Fig. 1A) and generates a small outflow channel. The 90 °C zone of the source pool is lined with a hard, 2- to 3-mm-thick, lustrous, metallic solid phase composed of sulfide minerals (Fig. 1B). A shelf of soft sediments is located on the eastern side of the spring and encompasses ~15% of the pool perimeter (Fig. 1 inset). These sediments are bathed in ~3–5 cm of water at temperatures ranging from 75–85 °C.

The two other sampling sites at Monarch Geyser and Cistern Spring (Norris Geyser Basin, YNP, UTMs (Easting/Northing) 523313/4952366 and 523439/4952232, respectively) were more acidic, but also representative of hypoxic sulfur sediment systems in YNP. Monarch Geyser (~4 m diameter) 'erupts' only intermittently, but exhibits episodic (sometimes 0.5 h frequency) water-level fluctuations of at least 5–10 cm, at a pH of ~4.2–4.4 (Fig. 1C) and temperatures ranging between 80–90 °C. The source pool of Cistern Spring (~5 m diameter) (Fig. 1D) exhibits variable pH values from 4.3–5.2 (McCleskey *et al.*, 2005) (pH 4.8–5.0 during sampling times reported here) and a temperature of ~82–86 °C. Both of the lower pH pools are lined with fine yellow sediments containing significant amounts of elemental sulfur (S^0). All three springs are hypoxic and contain elevated levels of total dissolved sulfide (~20 μM) and significant fractions of reduced sulfur minerals in the sediments. All springs are dominated by Na^+ and Cl^- (10–15 mM), with ionic strength values ranging from 15 to 25 mM (Table S1).

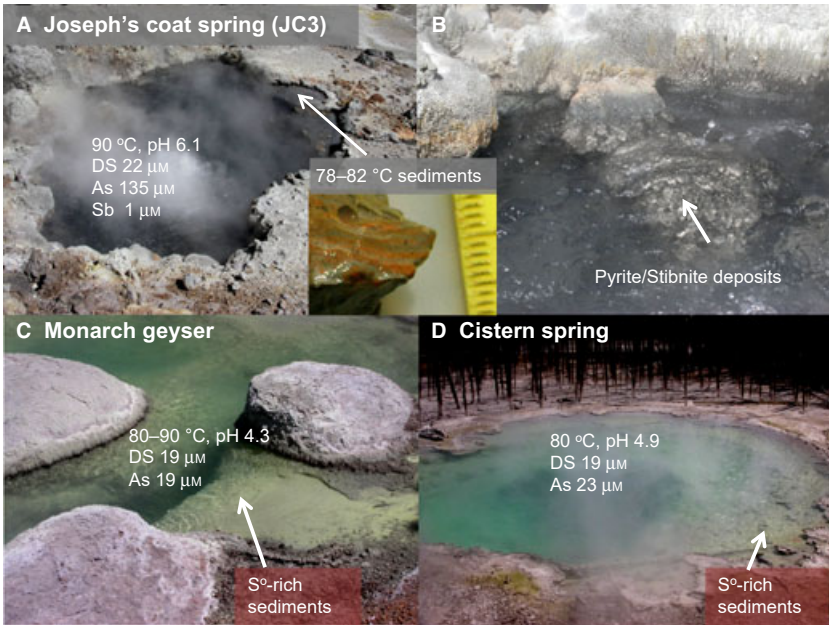

Fig. 1 Photographs of Joseph's Coat Hot Spring (JC3) (A,B), Monarch Geyser (C), and Cistern Spring (D) document sediment sampling locations and important geochemical attributes of these hypoxic, sulfidic systems (DS= total dissolved sulfide). Inset: Cross-section of 78–82 °C sediments collected from a shallow shelf on the southeastern edge of the JC3 source pool showing orange, yellow, and gray banding of sediments. Hatches on ruler are 1 mm. Photograph Dates: JC3 = July 28, 2004; MG and CS= May 21, 2008.

Extensive analyses of source-pool aqueous- and solid-phase geochemistry were conducted during multiple field trips to each of the sites. Microbial community composition (16S rRNA gene sequences) was also analyzed multiple times during this period. The Joseph's Coat site was characterized during five consecutive field trips during the summers of 2003–2007, and Monarch Geyser and Cistern Spring were sampled during 2006–2008.

Aqueous geochemistry

Springwater geochemistry was analyzed following protocols described previously (Inskeep *et al.*, 2005), although revised methods were implemented for dissolved gases in recent years. After 2005, dissolved oxygen (DO) was determined on-site using a Winkler protocol (APHA, 1998), with the modification that the initial reactions were conducted in a closed-headspace syringe. Briefly, a 60-mL syringe was filled with 60-mL sample and capped with a rubber septum to avoid any contact with the atmosphere. One-milliliter syringes were used to inject 0.4 mL of 2.15 M $MnSO_4$ and 0.4 mL of alkali-iodide-azide solution (12 M NaOH, 0.869 M KI, 0.15 M NaN_3), respectively, through the septa. The sample was inverted several times to mix the suspension and allowed to equilibrate for 3–5 min or until the resulting floc settled. This mixing and settling process was repeated before 0.4 mL of concentrated H_2SO_4 was added via another needle and syringe. The 60-mL syringe was inverted until the floc is completely dissolved, and then 30 mL of the mixture was titrated with sodium thiosulfate (0.0101 M) to quantify DO. Headspace gas chromatography (GC) was utilized to determine dissolved H_2, CH_4, and CO_2. Samples for dissolved gas analysis were collected using an inline 142-mm, 0.2 μM filter and peristaltic pump to fill 160-mL glass serum bottles. The bottles were purged with three pore volumes of sample and then capped with zero headspace using butyl stoppers. Dissolved gasses were analyzed, and concentrations were calculated as described previously (Inskeep *et al.*, 2005).

Thiosulfate concentration was determined using ion chromatography (Inskeep *et al.*, 2005) on samples collected using several protocols (Xu *et al.*, 1998). Aqueous samples from Monarch and Cistern were analyzed within 24 h. As the samples from JC3 were obtained in the backcountry, IC analysis was typically not completed until 5 days after sampling. Consequently, several different methods of sample storage were used. Aqueous samples were collected with no headspace in sealed serum bottles and stored at ~4 °C. Samples were also preserved in the field by adding 30 mL of spring water to 30-mL amber bottles containing 0.4 mL of 0.6 M $ZnCl_2$. One milliliter of 1 M NaOH was added to insure that all dissolved sulfide was fixed as ZnS, thus minimizing any conversion of sulfide to thiosulfate during sample storage (Xu *et al.*, 1998). Samples were filtered prior to IC injection to remove any ZnS precipitates. Polythionate analysis was also conducted using this same protocol plus the addition of 0.5 mL of 1 M KCN solutions (Xu *et al.*, 1998). The composition of the chromatographic peak with a retention time matching that of standard $S_2O_3^{2-}$ was verified by collecting 1-mL volumes with a fraction collector and analyzing these solutions with ICP-OES. The calculated sulfur concentration of the peak corresponded to the values expected for $S_2O_3^{2-}$, and no other elements such as arsenic (As) were detected in the fraction. Samples collected for thioarsenate

analyses were immediately frozen on dry ice. Thioarsenate concentrations were measured in samples collected in 2007 and 2008 using ion chromatography (Dionex DX500, Dionex Corp, Sunnyvale, CA, USA) coupled with ICP-MS detection as described by Planer-Friedrich *et al.* (2007) with the exception that the ICP-MS used was an Agilent 7500ce ICP-MS (As was monitored using the m/z = 75 line with the system operated in the helium mode to remove possible interferences by $ArCl^+$ adducts; analysis was performed at the MSU Environmental and Biofilm Mass Spectrometry Facility).

Solid-phase analysis and identification

The composition, structure, and mineralogy of solid phases present in each site were determined using a suite of analytical procedures including the following: (i) field emission scanning electron microscopy (FE–SEM; Zeiss Supra 55VP, Carl Zeiss, Inc., Oberkochen, Germany) coupled with small spot electron backscatter analysis (EBSD), (ii) acid digestion (HNO_3–$HClO_4$–HF at 110 °C) followed by elemental analysis with ICP-OES, (iii) X-ray diffraction at the Stanford Synchrotron Radiation Lightsource (SSRL), and (iv) X-ray absorption near-edge structure (XANES) and extended X-ray absorption fine structure (EXAFS) spectroscopy also at the Stanford Synchrotron Radiation Lightsource (SSRL).

Extended X-ray absorption fine structure (EXAFS) spectra for Sb were obtained on beamline 11-2 using an unfocused beam and a double-crystal Si(220) monochromator. Incident and transmitted intensity were measured using ion chambers, while X-ray fluorescence was measured using a 13-element Ge detector. Spectra were collected from −230 to 880 eV relative to the Sb K-edge of 30491 eV, and energy calibration was achieved via scanning dilute sample of sodium antimonite (Sb(III)). Sulfur XANES were collected at SSRL on beamline 6–2, equipped with a Si(110) monochromator. Samples were placed in a He-purged sample chamber, and scans were conducted in 0.15 eV increments from 50 eV below to 150 eV above the S K-edge (2472 eV) and in 1 eV increments thereafter. The inflection point of elemental sulfur was used for energy calibration at 2472 eV.

Antimony and S fluorescence were averaged and normalized to unity using the XAS data reduction software SIXPACK (Webb, 2005). SIXPACK/IFEFFIT algorithms were used to isolate backscattering contributions for Sb by subtracting a spline function from the EXAFS data region. The resulting function was then converted from units of eV to Å^{-1}, weighted by k^3, and windowed from 3–12 Å^{-1}. Linear combination of model compounds including sodium antimonite and stibnite was performed to reconstruct unknown spectra. Model compound contributions were deemed significant if their mole percentage was greater than 10%. First-derivative sulfur XANES spectra were utilized to identify inflection points indicative of specific sulfur species; first-derivative spectra of unknown samples were superimposed and compared with pyrite, amorphous iron sulfide, elemental sulfur, and sodium sulfate to determine S oxidation state.

Synchrotron X-ray powder diffraction was performed at 12735 eV at beamline 11-3 (SSRL), with an energy resolution ($\Delta E/E$) of $\sim 5\times10^{-4}$ equipped with a Si(311) monochromator and a MAR345 CCD detector. Finely crushed material was placed between two polycarbonate windows to a nominal thickness of 100 μM and mounted in an aluminum sample holder. Patterns were energy calibrated using a lanthanum hexaboride standard. Resulting powder diffraction images were radially integrated, converted to d-space vs. relative intensity, and analyzed for mineral phases using JADE 6.0 (Materials Data, Inc., Livermore, CA, USA).

Chemical speciation and thermodynamic calculations

The free-energy values (ΔG_{rxn}) of a set of oxidation–reduction reactions were calculated using predicted activities of chemical species obtained via aqueous equilibrium modeling (MINTEQ, ver 2.53, Allison *et al.*, 1991) and standard state Gibbs free-energy values (ΔG^o_{rxn}) corrected for temperature. The reactions are representative of a range of possible chemolithotrophic and chemoorganotrophic metabolisms. Most temperature-dependent ΔG^o_{rxn} values were obtained from Amend & Shock (2001), while thermodynamic data for reactions with dissolved and solid-phase Sb compounds were obtained from Fillella & May (2003). Values of ΔG^o_{rxn} not provided in Amend & Shock (2001) or other literature were calculated from temperature-corrected standard free energies of formation (ΔG^o_f). Measured values of total soluble chemical constituents were used as input to calculate the activities of chemical species at in situ temperatures with the aqueous equilibrium model, Visual MINTEQ (Ver 2.53, Allison *et al.*, 1991).

Microbial community 16S rRNA genes and phylogenetic analysis

Analysis of 16S rRNA gene sequences from sediment samples collected in 2005 and 2006 was used to assess the composition and diversity of microbial populations. Sediments (0–5 mm) were collected in sterile 50-mL conical bottom polyethylene tubes tubes utilizing aseptic techniques and immediately placed on dry ice for transport to a −80 °C freezer. The FastDNA SPIN Kit for soil (Q-Biogene, Irvine, CA, USA) was used to extract total DNA from the samples, which served as template for PCR of 16S rRNA genes using both *Bacteria*-specific [Bac8f (5′-AGAGTTTGATCCTGGCTCAG-3′)] and *Archaea*-specific

[Arc2f (5′-TTCCGGTTGATCCYGCCGGA-3′) forward primers coupled with the universal reverse primer Univ1392r (5′-ACGGGCGGTGTGTAC-3′). Purified PCR products were cloned using the pGEM-T Vector System (Promega Corp., Madison, WI, USA), and the inserts were sequenced using T7P and SP6 primers (TGEN, Phoenix, AZ, USA). Chimeras were detected with Mallard software (Ashelford *et al.*, 2006). DNA sequences were edited using the Sequencher program (v.4.5; Gene Codes Corp, Ann Arbor, MI, USA), and sequences were deposited in the GenBank database. Alignments were performed in MEGA 4.0.2 (Build #4028; Tamura *et al.*, 2007) using ClustalW set to default values and then manually edited. Trees were constructed using the neighbor-joining method and maximum composite likelihood model within MEGA.

Isolation and characterization of a S-respiring Thermoproteales

Sediment samples (~78 °C) were collected from the shallow shelf located on the east side of the source pool of JC3 (August 2006) using a sterile 60-mL syringe and injected immediately into a sterile 40-mL serum bottle. The serum bottle was filled with spring water, capped with no headspace, and stored at ambient temperatures (17–23 °C) for 5 days. Samples of the sediment suspension (0.5 mL) were used as inoculum into 10-mL serum bottles containing 5 mL of synthetic growth medium and serially diluted to 10^{-7} in triplicate. The serum bottles were incubated at 75 ± 2 °C without shaking. The synthetic growth medium used for cultivation of anaerobic thermophiles contained 4.4 mM KCl, 6.2 mM NH_4Cl, 2.4 mM KH_2PO_4, 1.62 mM $MgCl_2$, 2.2 mM $CaCl_2$, 2.1 mM Na_2S, 1 g L^{-1} starch, 0.2 g L^{-1} yeast extract (Difco), 15 μg mL^{-1} kanamycin, 15 μg mL^{-1} vancomycin, 1 mL L^{-1} trace element solution (Pfenning & Lippert, 1966), 1 mL L^{-1} vitamin solution (Wolin *et al.*, 1963), 1 mg L^{-1} resazurin, and 0.05 g L^{-1} elemental sulfur. Medium pH was adjusted to 7.0 with HCl or NaOH before addition to serum bottles. The headspace (5 mL) was purged with 99.96% N_2 (g) for 30 min prior to addition of 100 μL of 0.1 M cysteine to scavenge remaining O_2. The addition of cysteine lowered the pH to ~6.0. Kanamycin and vancomycin were added to inhibit bacterial growth. These culture conditions were designed to be consistent with hypoxic sediments of JC3 and targeted micro-organisms capable of heterotrophic growth and respiration on elemental S.

Cultures were examined using fluorescence microscopy after staining with an equal volume of 10x SYBR Green I (Molecular Probes, Eugene, OR, USA) for 15 min and then heat fixing (75 °C) 10 μL of the suspension placed on a glass slide. A Zeiss Axioskop 2 + fluorescent microscope (Carl Zeiss, Inc.) was used to identify morphology, to confirm isolate purity, and to monitor growth (cell numbers). The concentration of dissolved H_2S was measured using a modified version of the amine–sulfuric acid method (APHA, 1998). The modified low-volume method utilized 33 μL of amine–sulfuric acid reagent and 10 μL of $FeCl_3$ reagent mixed in a 1.5-mL centrifuge tube. A 50-μL aliquot of sample was injected beneath the surface of the mixture to minimize loss of H_2S, followed by addition of 450 μL of deionized H_2O. Blanks received 500 μL of H_2O. Dihydrogen phosphate reagent (3.79 M H_2PO_4) was added (107 μL), and the tubes were vortexed for 30 s and then centrifuged at 13 000 × g for 1 min to pellet any precipitates. The supernatant was used to measure absorbance at 664 nm. The most dilute bottles showing H_2S production were transferred to the same medium and serially diluted to 10^{-7}.

A pure culture of rod-shaped cells was obtained after several cycles of dilution to extinction. Culture purity was tested by PCR amplification, cloning, and sequencing of 16S rRNA genes. Universal bacterial primer sets as well as multiple terminal and internal universal archaeal primers were used to confirm culture purity. Fifty clones were prepared using primer sets that generated product, and the clones were sequenced. Phylogenetic analysis revealed that the isolate (strain WP30) was most closely related to *Pyrobaculum arsenaticum* and *Thermoproteus neutrophilus* (98% nucleotide identity; Huber *et al.*, 2000; Fischer *et al.*, 1983). Unless otherwise stated, further growth experiments with strain WP30 were conducted in standard synthetic medium under a N_2 (g) atmosphere at 75 °C. Growth curves were generated in triplicate at pH 6.0 and 0.2 g L^{-1} yeast extract. Bottles used for growth curve experiments were initially inoculated with 10^3 cells mL^{-1}. Growth was monitored by direct counting (cells mL^{-1}) and by measuring dissolved sulfide concentrations using the low-volume sulfide method described previously. The pH optimum of strain WP30 was determined at 75 °C (in triplicate) by adjusting the pH of the growth medium with either HCl or NaOH after the addition of 5 mM HEPES, 5 mM MES, and 10 mM H_3BO_3 buffers to obtain 7 pH values ranging from 4 to 10. After 5 days, H_2S concentrations, cells numbers, and final pH were determined. The maximum pH variation between initial and final measurements was <0.3 pH units.

The ability of strain WP30 to utilize various substrates as a carbon and energy source was evaluated and included D-glucose (J.T. Baker Chemical Co., Phillipsburg, NJ, USA), lactose (Sigma-Aldrich Chemical Co., Milwaukee, WI, USA), soluble starch (Sigma-Aldrich Chemical Co.), and acetate (J.T. Baker Chemical Co.) added at 0.2 g L^{-1}. Various amounts of yeast extract (YE) and tryptic soy broth (TSB) were also tested to ascertain potential carbon and energy sources for strain WP30 (0.0, 0.002, 0.02, and 0.2 g L^{-1}). To check for autotrophic growth, a mixture of 50% CO_2 (g) and 50% H_2 was used as headspace in the

absence of any organic carbon sources (however, a trace amount of YE (0.002 g L^{-1}) shown to be required for growth was also included). The ability to ferment YE was determined by the addition of 0.2 g L^{-1} YE to the medium, while all other potential electron acceptors were excluded (i.e., nitrate, sulfate, sulfur). Possible electron acceptors other than elemental S^0 were tested by excluding S^0 from the medium and adding either Fe(III) (0.02 g L^{-1}) as Fe_2O_3 (hematite with minor amounts of other Fe oxyhydroxide phases; particle size < 1 μM; J.T. Baker Co.) or Sb^V (0.02 g L^{-1}) as Sb_2O_5 (Acros Organics, Fair Lawn, NJ, USA), NO_3^- (10 mM), or $S_2O_3^{2-}$(10 mM). To test for growth under micro-aerobic conditions, one milliliter of sterilized air (per 5-mL headspace) was injected into inoculated serum bottles, creating a ~4% O_2 headspace environment.

Amplification of a *sreA*-like gene

Because it was determined that strain WP30 can grow under anaerobic conditions using S^0 as an electron acceptor, efforts were taken to identify a possible sulfur reductase (*sreA*) gene. SreA proteins are molybdopterins that have been shown to be important for respiration on S^0 in *Acidianus ambivalens* (Laska *et al.*, 2003) and *Aquifex aeolicus* (Gurial *et al.*, 2005) and may play an important role in S^0 respiration by strain WP30. Degenerate primers designed using putative *sreA*-like sequences in *Thermofilum pendens*, *Thermoproteus neutrophilus,* and *Pyrobaculum* spp. were used to amplify an *sreA*-like sequence in *Pyrobaculum* strain WP30. The primers TTP*sreA* forward (5′–SWRGARGTSGACTGGGA–3′) and TTP*sreA* reverse (5′–GYRTACCAYCCRTCYTC–3′) were used at a concentration of 1 μM. The PCR protocol consisted of 95 °C for 2 min, 32 cycles of 95 °C for 45 s, 50 °C for 45 s, 72 °C for 50 s, and final extension of 72 °C for 5 min. To verify that the correct target sequence was amplified, purified PCR products were cloned and sequenced.

RESULTS AND DISCUSSION

Aqueous geochemistry and solid-phase mineralogy

The three hypoxic geothermal systems examined in this study have source waters > 85 °C and contain high concentrations of reduced inorganic constituents including total dissolved sulfide (19–22 μM), thiosulfate (20–890 μM), arsenite (~20–120 μM), ammonium (0.1–6.2 mM), CH_4(aq) (0.3–0.8 μM), and H_2(aq) (0.1–0.4 μM; Table S1). Joseph's Coat Spring contains appreciably higher concentrations of thiosulfate (890 ± 300 μM), total soluble arsenic (135 μM), antimony (0.8 μM), and ammonium (6.2 mM) than Monarch Geyser or Cistern Spring, and to date, these are the highest measured aqueous concentrations of thiosulfate, arsenic, and antimony in YNP. Comparisons of different sample preservation methods for thiosulfate analyses did not result in significant differences in thiosulfate concentrations. Polythionate was not detected in any of the springs (DL ~10 μM). The high ammonium in JC3 is consistent with other geothermal springs in this region and is thought to originate from the distillation of buried marine sediments (Fournier, 2005; Holloway *et al.*, 2011). Dissolved H_2 concentrations were ~3 times higher in Monarch and Cistern (~300 nM) compared with JC3 and are among the highest concentrations of dissolved H_2 measured in terrestrial hot springs of YNP (Inskeep *et al.*, 2005; Spear *et al.*, 2005; Ackerman, 2006). Although thioarsenates were detected in JC3 (6 μM, primarily as dithioarsenate), they represented only about 4% of the total dissolved arsenic in the system.

The sediments sampled from each source pool all contain elemental sulfur, either as rhombohedra and/or spheres ranging in diameter from ~5–75 μM, as determined using scanning electron microscopy (SEM and/or FE-SEM; Fig. 2). The formation of elemental sulfur in these environments is thought to be controlled by the oxidation of H_2S(aq) via a pH-dependent disproportionation mechanism involving thiosulfate (Xu *et al.*, 1998, 2000). The formation of elemental sulfur is favored at lower pH due to the higher concentration of H_2S vs. HS^-, and this may be one explanation for the greater abundance of elemental S in Monarch and Cistern compared with JC3, as well as the greater apparent stability of thiosulfate in the JC3 system. Elemental S was a dominant phase in sediments from Monarch Geyser and Cistern Spring, comprising up to 90% of the mineral fraction in these systems (SEM-EDAX and synchrotron XRD, Fig. S1).

The higher aqueous concentrations of arsenic and antimony combined with higher pH at JC3 (pH 6.0 vs. 4.3–4.9) result in the formation of sulfide minerals including amorphous FeS, framboidal FeS_2 (pyrite), Sb_2S_3 (stibnite), and As_2S_3 (orpiment). The metallic, 1–2-mm-thick solid phase forming in the hottest zone (90 °C) of this source pool is comprised almost entirely of pyrite (FeS_2) and stibnite (Sb_2S_3) (Fig. 2A–C, Fig. S2). A white solid phase found immediately underneath the 1- to 2-mm metallic phase was identified via XRD to be >99% SiO_2 (Fig. S1). Sediments accumulating along the edges of the source pool (78–82 °C) are comprised primarily of SiO_2 with evidence of FeS_2, Sb_2S_3, S^o As_2S_3, and alunite ($KAl_3(SO_4)_2(OH)_6$). SEM images from JC3 reveal what are likely micro-organisms in close association with pyrite and elemental sulfur phases (Fig. 2B,D). Orange–yellow banding patterns observed beneath a 0.5–1-mm layer of fine, gray pyritic sediment (Fig. 1 inset) were analyzed using SEM-EDAX and found to be associated with zones enriched in either orpiment (yellow) or stibnite (orange).

Analytical results using synchrotron X-ray diffraction (XRD) and X-ray absorption near-edge spectroscopy

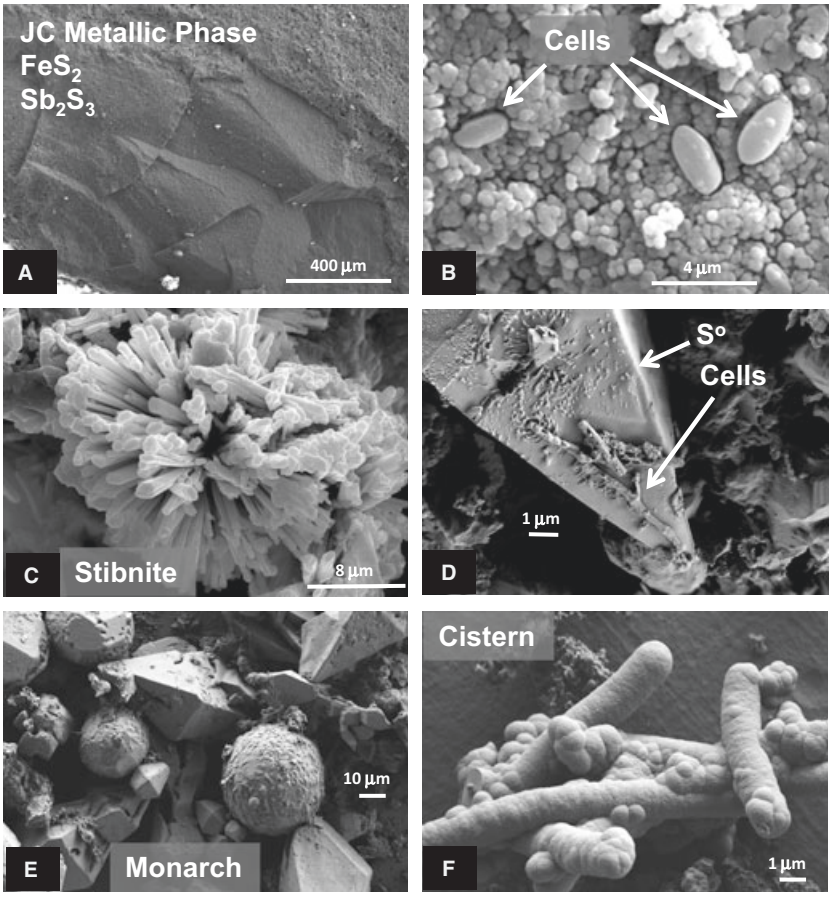

Fig. 2 Scanning electron micrographs (SEM) of source-pool mineral deposits from Joseph's Coat Hot Spring (JC3), Monarch Geyser (MG), and Cistern Spring (CS). (A) Low magnification (70X) image from JC3 shows top surface (cross-section) of the ~2-mm-thick sulfide mineral deposit comprised of pyrite and stibnite; (B) higher magnification (7500X) image reveals what may be individual cells that resemble *Geothermobacterium ferrireducens* (Kashefi *et al.*, 2002) imbedded within framboidal pyrite; (C) highly structured stibnite crystals (confirmed by EBSD) formed on the pyrite surface; (D) filamentous organisms on sulfur rhombohedron collected from JC3 sediments; (E) a variety of elemental sulfur morphologies found in Monarch sediments; and (F) filamentous cells from Cistern Spring sediments encrusted with solid-phase SiO_2.

(XANES) show that the metallic phase formed at near 90 °C in JC3 exhibits diffraction peaks consistent with pyrite and stibnite, and predominant oxidation states of sulfur and antimony of –I and + III, respectively (Fig. 3). Sulfur XANES of the JC3A metallic sample show a predominance of reduced sulfur phases, with a major peak at the nominal oxidation state of (−I) indicative of pyrite and a shoulder at (−II) consistent with stibnite. The corresponding first-derivative antimony XANES spectra, while broad due to prolonged K-shell core-hole lifetime, illustrate a dominance of reduced antimony (as stibnite) within the JC3A metallic sample.

The edges of the JC3 source pool accumulate sediments in slightly cooler (72–85 °C) environments, and XRD patterns are dominated by various phases of SiO_2 (Fig. S1). Although not detected consistently in XRD runs, alunite, orpiment, elemental S, FeS, and Sb_2S_3 phases were all confirmed directly using SEM/EDAX of sediments from 78–82 °C. Total dissolution of these solid phases confirms a stibnitic, pyritic signature, but the total antimony and iron in sediments drop from 18–20% (w/w) in the metallic phase to near 1% in the sediments. Although the sediment samples are dominated by reduced sulfur at an apparent oxidation state of S(−I), a shoulder toward S(0) is apparent as well as a significant S(VI) peak consistent with the direct observation of alunite ($KAl_3(SO_4)_2(OH)_6$) in the sediment sample (Fig. 3). The antimony XANES spectra also show a significant increase in Sb(V) in the sediment sample compared with the metallic, stibnitic phase (Fig. 3). Although not shown, arsenic XANES spectra suggest that the majority of solid-phase arsenic in sediment samples has a nominal oxidation state of +III consistent with orpiment-like phases observed using SEM/EDX.

Calculation of aqueous saturation indices at spring temperatures {SI = log [ion activity product (IAP)/solubility product (K_{sp})]} with respect to known minerals (Table S3; Visual MINTEQ; Allison *et al.*, 1991) was performed to evaluate possible agreement with direct observations of specific solid phases. The JC3 source waters are significantly oversaturated with respect to Fe(III) oxide phases, slightly oversaturated with respect to amorphous quartz, and undersaturated with respect to FeS, As_2S_3, Sb_2S_3, and alunite (SI = −3.9,−7.8,−13.6, and−3.6, respectively). Although the presence of $SiO_2(s)$ phases is consistent with oversaturation indices, other sulfide minerals are not in apparent equilibrium with the aqueous phase, and these solids would not be predicted without a surface-catalyzed or biologically catalyzed process (e.g., Handley *et al.*,

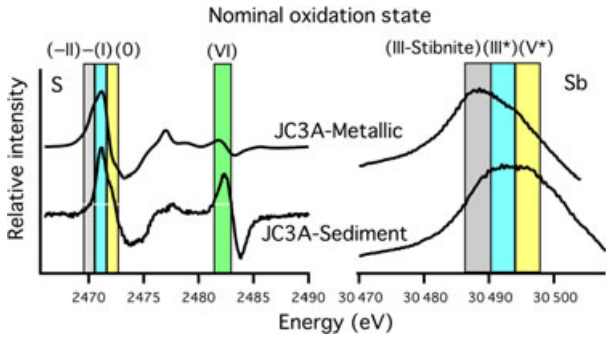

Fig. 3 First-derivative sulfur (*left*) and antimony (*right*) XANES spectra of JC3A metallic and sediment samples. Oxidation states marked with an asterisk (*) were calibrated with oxyanions of antimony (Na antimonate and Na antimonite).

2005). Furthermore, while these calculations were made using data from aqueous samples collected above the sediments, they may not accurately reflect concentrations of constituents in immobile water domains such as boundary layers around particles. The nucleation of solid phases from undersaturated conditions could be due in part to higher concentrations in those micro-environments. X-ray diffraction (XRD) patterns from Monarch and Cistern sediments (80 °C) were dominated by elemental sulfur and SiO_2 phases (Fig. S1).

The absence of measureable DO is consistent with the presence of dissolved sulfide and the ubiquity of reduced sulfur solid phases present in each of the geothermal systems studied. These results suggest that organisms present in these microbial communities are limited to extremely low levels of oxygen and/or utilize more reduced substrates as primary electron acceptors. Likely candidate electron acceptors in these systems include elemental sulfur, thiosulfate (0.02–0.9 mM), and sulfate (0.8–4.1 mM). Additional electron acceptors such as nitrate (8-18 μM), arsenate (4–22 μM), Fe(III) (0.2 μM), and dissolved oxygen (< 0.3 μM) are also energetically favorable under spring conditions (Table S2).

Microbial community composition

Bacterial and archaeal 16S rRNA gene sequence libraries from each of the solid-phase sediment samples reveal that these systems are dominated by relatively few genera (Figs 4 and 5). Phylogenetic analyses of long-fragment (>1200 bp) 16S rRNA gene sequences reveal that the dominant archaea in these hypoxic, sulfidic high-temperature environments are related to organisms within the orders Thermoproteales and Desulfurococcales (phylum Crenarchaeota), as well as the candidate phylum Thaumarchaeota (Brochier-Armanet *et al.*, 2008). Of the ~200 archaeal 16S rRNA sequences characterized from these sites, nearly all (~90%) were related to either *Vulcanisaeta distributa* (94–98% nucleotide identity), *Acidilobus sulfurireducens* (92–99%), or *Thermofilum pendens* (87–97%). All of these isolated relatives are known sulfur-respiring hyperthermophiles (Zillig *et al.*, 1983; Itoh *et al.*, 2002; Boyd *et al.*, 2007; respectively). *Acidilobus*- and *Vulcanisaeta*-like sequences were the two most abundant clone groups observed in JC3 (91% total clones) and Monarch (89%) sediments, whereas Cistern sediments contain abundant *Thermofilum*-like populations (55%) in addition to the *Acidilobus*- and *Vulcanisaeta*-like sequences (Fig. 4). *Thermofilum*-like organisms were also abundant in JC3 where they accounted for 8% of the total archaeal clones. Other minor groups detected in these microbial communities were distantly related to *Fervidococcus fontis* (< 92% nucleotide identity), a Desulfurococcales isolated from the Uzon Caldera (Perevalova *et al.*, 2008), and other Thermoproteales group more closely related to *Pyrobaculum/Thermoproteus* spp. (93–98%; Huber *et al.*, 2006).

The metabolism of Desulfurococcales and Thermoproteales isolates whose relatives were detected in these sulfidic sediments involves utilization of complex organic substrates (e.g., peptides, yeast extract) as a carbon and electron donor, and elemental sulfur and/or thiosulfate ($S_2O_3^{2-}$) as an electron acceptor (e.g., Zillig *et al.*, 1983; Itoh *et al.*, 2002; Huber & Stetter, 2006; Huber *et al.*, 2006; Boyd *et al.*, 2007). The predominant phenotype observed in cultivated relatives is consistent with the geochemical attributes of these geothermal systems, suggesting that elemental sulfur and/or other reduced sulfur species play a central role in the survival and distribution of indigenous Desulfurococcales and Thermoproteales populations in YNP.

While members of the candidate phylum Thaumarchaeota were detected in both Monarch and Cistern Springs (clone groups BW258 and BW160), these organisms are only distantly related to cultivated relatives (<88% nt identity) and represent uncharacterized taxonomic groups (perhaps order, class, or subphylum within this phylum). Consequently, inferring the metabolic capabilities of these less-dominant organisms is too speculative at the current time, other than obvious possible associations with transformations of sulfur, nitrate reduction, and/or heterotrophic growth at high temperature (Beam *et al.*, 2011). Although many currently isolated Thaumarchaea oxidize ammonia, no *amo*A genes were noted in metagenome studies of these sites (Inskeep *et al.*, 2010; Jay *et al.*, 2011).

The only bacterial sequences detected in the metallic phase lining the JC3 source pool (88–90 °C) were all highly related to *Geothermobacterium ferrireducens* (99% nucleotide identity; Fig. 5). The metabolism of this obligate anaerobe (obtained from Obsidian Pool, YNP) requires H_2 as an electron donor and Fe(III) as an electron acceptor (Kashefi *et al.*, 2002), which is consistent with the production of Fe(II) and mineralization of pyrite (FeS_2) observed in JC3. The *Geothermobacterium*-like organism(s)

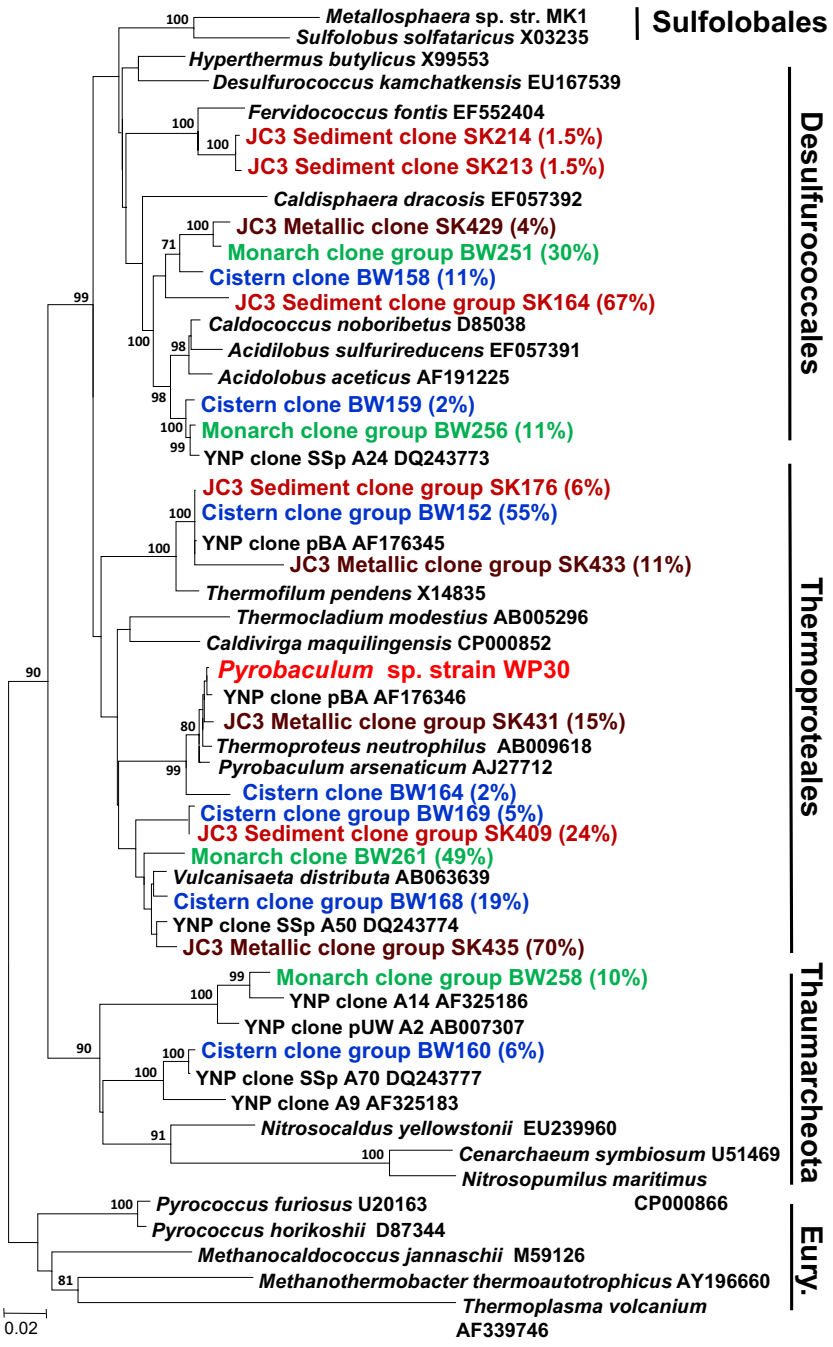

Fig. 4 Neighbor-joining phylogenetic tree created with near-full-length archaeal 16S rRNA gene sequences detected in Joseph's Coat Spring (JC3 metallic brown font and JC3 sediment red font), Monarch Geyser (green font), and Cistern Spring (blue font), and related micro-organisms [taxonomic clades are indicated; scale bar = 0.02 substitutions per sequence position; bootstrap values per 1000 replicates; percentages (in parentheses) are calculated from the number of closely related 16S rRNA gene sequences divided by the total number of clones sequenced for each site; *Aquifex pyrophilus* (M83548) was used as the outgroup (not shown)]. The total number of sequenced clones for each site was as follows: JC3 metallic = 27, JC3 sediment = 79, Monarch = 47, and Cistern = 47.

were also found in the cooler sediments of JC3 (~80 °C) along with members of the Aquificales related to *Thermocrinis* spp. (~99% nt identity; Fig. 5). Cultured *Thermocrinis* spp. require H_2, elemental sulfur, or thiosulfate for growth under aerobic to micro-aerobic conditions (Huber *et al.*, 1998; Eder & Huber, 2002), suggesting that low levels of oxygen may be available in lower temperature sediments at 80 °C. The high levels of H_2(aq) and reduced sulfur species in JC3 (Table S1) make it difficult to infer definitive electron donors and acceptors for chemolithotrophy or chemoorganotrophy, especially considering that many possible exergonic reactions involving these species could support metabolism (Table S2). Sequences highly related to *Geothermobacterium* and *Thermocrinis* were also detected in Cistern Spring (Fig. 5) where the pH ranged from 4.4–5.2; however, no Fe solid phases are present to suggest that the *Geothermobacterium*-like organisms might be involved in Fe (III) reduction and biomineralization. Although the temperature of Monarch sediments (78–80 °C) was similar to samples from JC3 and Cistern, no bacterial 16S rRNA gene sequences were amplified from these samples, despite repeated attempts with different universal bacterial primers

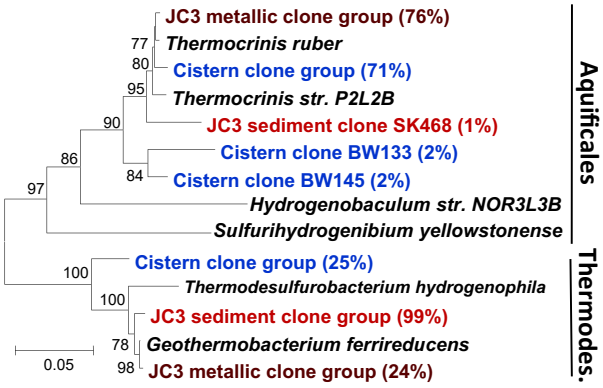

Fig. 5 Neighbor-joining phylogenetic tree created with bacterial 16S rRNA gene sequences detected in Joseph's Coat Spring (JC3 metallic brown font and JC3 sediments red font) and Cistern Spring (blue font), and related micro-organisms [taxonomic clades indicated; scale bar = 0.05 substitutions per sequence position; bootstrap values per 1000 replicates; Thermodes. = Thermodesulfobacteriales; percentages (in parentheses) are calculated from the number of closely related 16S rRNA gene sequences divided by the total number of clones sequenced for each site; *Candidatus* Korarchaeum *cryptofilum* was used as the outgroup (not shown)]. The total number of sequenced clones for each site was as follows: JC3 metallic = 25, JC3 sediment = 98, and Cistern = 48.

that worked efficiently in other similar sulfidic sediments (i.e., Cistern, JC3, as well numerous other geothermal samples not reported here).

Characterization of a Thermoproteales isolate from YNP

An anaerobic Thermoproteales isolate (referred to here as *Pyrobaculum* sp. strain WP30) was cultured from 78 °C sediments retrieved from JC3 after several cycles of dilution to extinction in serum bottles containing elemental sulfur, yeast extract, and background synthetic medium under a N_2(g) headspace. The near-full-length 16S rRNA gene sequence (1380 bp, GenBank Accession Number: 1547525) of the isolate is highly related to one of the important 16S rRNA clone groups observed in JC3 (Fig. 4) and is ~98% identical (nt) to either *Thermoproteus neutrophilus* or *Pyrobaculum arsenaticum* (Fischer *et al.*, 1983; Huber *et al.*, 2000). A 748-bp protein encoding intron was located at position 917 (*E. coli* numbering) of the WP30 16S rRNA gene. The closest known intron near this position is the Cma-II intron in *Caldivirga maquilingensis* that is located 8 bp upstream (Itoh *et al.*, 2003). While the nucleotide sequence of the WP30 intron is not closely related to current sequences in public databases, the deduced protein shares 31% amino acid identity to the homing endonuclease characterized in the 16S rDNA gene of *Aeropyrum pernix* (Nomura & Sako, 1998). Considering this region forms a conserved hairpin structure, the intron may be accessible for excision by the translated endonuclease (Baker & Cowan, 2004).

Morphological characteristics of strain WP30 are similar to other members of the Thermoproteales. Specifically, strain WP30 is a rod-shaped organism (~0.5 μM diameter, 3–5 μM length) with infrequent branching, arranged in aggregates, and often attached to elemental sulfur particles (Fig. 6A). Approximately 10% of cells exhibited globular bodies toward the end of exponential growth phase, similar to the *golf club* features formed by *Thermofilum pendens* (Zillig *et al.*, 1983), *Thermocladium modestius* (Itoh *et al.*, 1998), *Caldivirga maquilingensis* (Itoh *et al.*, 1999), and *Pyrobaculum aerophilum* (Volkl *et al.*, 1993). Sulfide production by WP30 correlated with cell growth (Fig. 6B), although maximum total dissolved sulfide (DS) concentrations were observed after cells reached stationary phase (1.3 mM DS after 14 days). Maximum cell densities of 7.8 × 10^6 cells mL^{-1} were achieved using optimized growth conditions (pH 6.1, 75 °C, 0.2 g L^{-1} yeast extract) representing doubling times of 12.6 h. Growth of strain WP30 occurred over a temperature range of 60–94 °C and a wide pH range of 3.6–9.0, but maximum cell densities were achieved at 75 °C (Fig. 6C) and at pH values of 4.6–6.6 at 75 °C (Fig. 6D). The optimal temperature and pH of strain WP30 corresponds well with the sediment environment from which the isolate was obtained (T = 78 °C, pH = 6.1).

Strain WP30 grows under strictly anaerobic conditions using elemental sulfur or arsenate as an electron acceptor and yeast extract as a carbon and energy source (Table S4). Minor growth was observed using H_2(g) in the headspace (50%); however, no growth was detected when Fe(III) or nitrate (NO_3^-) was supplied as electron acceptors. However, the strain has not been thoroughly evaluated on a range of Fe(III) solids with varying bioavailability. A novel putative sulfur reductase (*sreA*) gene was identified in *Pyrobaculum* strain WP30 using a degenerate primer set designed from putative *sreA* sequences in *T. pendens*, *Thermoproteus neutrophilus*, and *Pyrobaculum* spp. SreA proteins have been characterized in *Acidianus ambivalens* (Laska *et al.*, 2003) and *Aquifex aeolicus* (Gurial *et al.*, 2005) and have been shown to be important components of a multi-protein complex utilized for respiration on elemental sulfur. Final cell densities and growth rates of strain WP30 were directly correlated with initial YE concentration, whereas lactate, acetate, starch, and glucose did not enhance growth of WP30 under low levels of YE (0.002 or 0.02 g L^{-1}), nor did these substrates support significant growth in the absence of YE.

Sulfur transformations in high-temperature sulfidic springs

Numerous oxidation–reduction reactions involving sulfur species are thermodynamically favorable in these geothermal systems (Table S2), some of which may be mediated

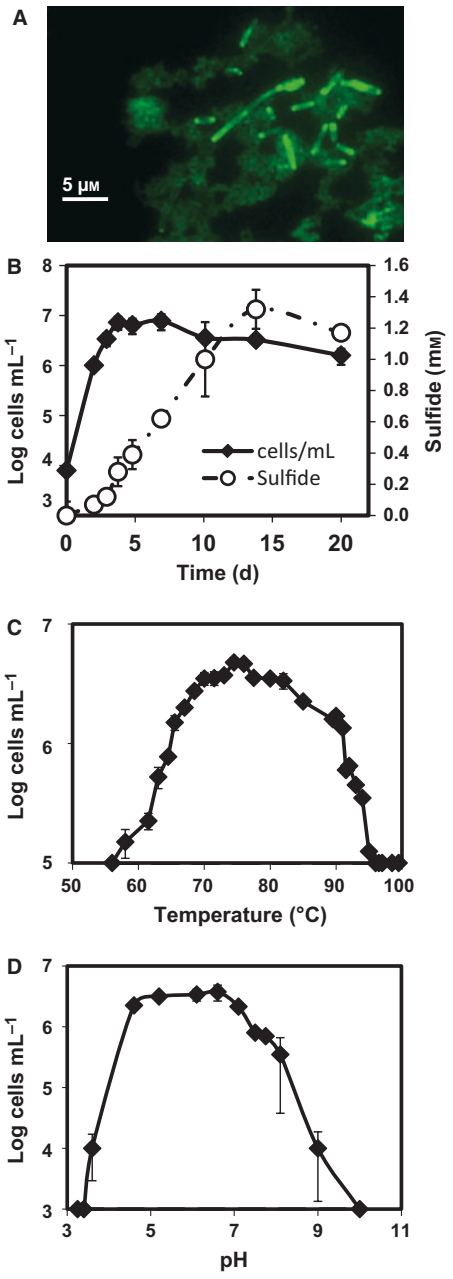

Fig. 6 (A) Image of *Pyrobaculum* sp. strain WP30 cells attached to elemental sulfur particles obtained using SYBR green, and (B) growth (cells mL^{-1}) of *Pyrobaculum* sp. strain WP30 at optimum temperature and pH (75 °C, pH 6.1) plotted with concentrations of total dissolved sulfide as a function of time for triplicate samples. (C–D) Growth of strain WP30 as a function of temperature (assessed after 5 days at pH 6.1) and pH (assessed after 5 days at 75 °C).

by micro-organisms or occur abiotically at rapid rates (Xu *et al.*, 1998, 2000). As reduced geothermal source waters containing dissolved sulfide (e.g., H_2S(aq), HS^-) interact with atmospheric oxygen, a myriad of possible sulfur species can result from abiotic and/or biotic oxidation of H_2S/HS^-(aq) including polysulfide (S_n^{2-}), thiosulfate ($S_2O_3^{2-}$), trithionate ($S_3O_6^{2-}$), tetrathionate ($S_4O_6^{2-}$), polythionate ($S_nO_6^{2-}$), and sulfite (SO_3^{2-}). This leads to a staggering number of possible exergonic reactions that could theoretically support microbial metabolism (Amend & Shock, 2001; Pronk *et al.*, 1990; Blumentals *et al.*, 1990; Jorgensen, 1990; Vairavamurthy *et al.*, 1993; Inskeep *et al.*, 2005). The high concentrations of thiosulfate in JC3 and Cistern make it an especially important electron donor and/or acceptor, depending on the redox couple envisioned and the organism involved (Table S2). For example, strain WP30 and other *Pyrobaculum* relatives (Huber *et al.*, 2006) can utilize $S_2O_3^{2-}$ and/or elemental S as an electron acceptor under anaerobic conditions, whereas cultured *Thermocrinis* spp. are capable of using thiosulfate as an electron donor under micro-aerobic conditions (Huber *et al.*, 1998; Eder & Huber, 2002).

The majority of archaeal 16S rRNA gene sequences obtained from the high-temperature environments of JC3, Monarch, and Cistern are related to chemoorganotrophic sulfur reducers (Huber & Stetter, 2006; Huber *et al.*, 2006; Boyd *et al.*, 2007). Consequently, elemental sulfur plays a pivotal role in the bioenergetics of hypoxic sulfidic sediments. Direct microscopic examination of spring sediments suggests that cells exist in close association with elemental sulfur rhombs (Fig. 2D). Moreover, WP30 cultures stained with SYBR green also reveal cell attachment to elemental sulfur particles (Fig. 6A). Although physical contact is considered to be important for many organisms that gain energy from elemental sulfur due to its very poor solubility (Boulegue, 1978; Zillig *et al.*, 1983), solubilization of elemental sulfur by unattached cells via electron shuttles has also been proposed (Druschel *et al.*, 2008). Moreover, micro-organisms can play an important role in the mineralization or dissolution of elemental sulfur and sulfide minerals (Huber *et al.*, 1989; Donald & Southam, 1999; Rawlings, 2002). Mineral saturation indices (Table S3) calculated from the activities of aqueous chemical species in the source pools of JC3, Cistern, and Monarch were all considerably undersaturated with respect to FeS, stibnite, and orpiment, suggesting that spontaneous nucleation would not be occurring at these ion concentrations. Conversely, it is possible that other surfaces (especially of biotic origin) may be important in nucleating and promoting crystal growth of these reduced mineral phases (Phoenix *et al.*, 2005). Alternatively, specific organisms may be directly involved in mediating a particular step important for solid-phase mineralization. For example, the closest relative of the *G. ferrireducens*-like organism detected in JC3 reduces Fe(III) to Fe(II) (Kashefi *et al.*, 2002), and consequently, this population may play an important role in the mineralization of pyrite in this system. This idea is supported by microscopic observations showing cells that resemble *G. ferrireducens* (Kashefi *et al.*, 2002) imbedded in the framboidal pyrite phase of JC3 (Fig. 2B). Moreover,

sulfur-reducing organisms detected and isolated from the JC3 sediments (e.g., *Pyrobaculum* strain WP30) produce copious amounts of dissolved sulfide, further promoting an environment favorable for the formation of sulfide minerals, including pyrite, stibnite, and orpiment.

The free-energy yields of reactions involving the reduction of elemental sulfur to sulfide (e.g., ~24 kJ mol electron^{-1} utilizing acetate) are low relative to many inorganic donor/acceptor processes and are similar when either H_2 or reduced carbon serves as the electron donor (Table S2; Rogers & Amend, 2006). Total dissolved organic carbon (DOC) concentrations in these springs range from 55 to 65 μM. Consequently, it is possible that anaerobic organisms present in these systems are dependent on reduced forms of carbon contributed exogenously or those produced by autotrophic organisms. The possible autotrophic organisms in these communities include relatives of *G. ferrireducens* and *Thermocrinis* spp.; however, our estimates of community composition using metagenomics (Jay *et al.*, 2011) suggest that bacteria are less abundant than the archaeal populations in these anaerobic sulfur sediments. It is certainly possible that one or more of the Desulfurococcales or Thermoproteales populations present in these sediments are capable of fixing CO_2 as a sole carbon source, and new autotrophic pathways have been proposed in both these crenarchaeal orders (Jahn *et al.*, 2007; Ramos-Vera *et al.*, 2009; Berg *et al.*, 2010). However, it is also possible that the relatively high concentrations of organic carbon found in these springs (~60 μM) may not be advantageous for autotrophic organisms. Current metagenome sequence analysis at these locations suggests that these hypoxic sulfidic sediments of YNP are dominated by crenarchaea of the Desulfurococcales and Thermoproteales that exhibit incomplete evidence for pathways required for the fixation of carbon dioxide (Inskeep *et al.*, 2010; Jay *et al.*, 2011). Moreover, numerous cultivated representatives of these lineages, as well as the isolate reported in the current study, all require complex carbon sources and respire elemental sulfur and/or thiosulfate. The role of these lineages in the evolutionary history of microbially mediated sulfur cycling among prokaryotes provides an interesting and fruitful area for further research.

ACKNOWLEDGMENTS

Authors appreciate assistance from G. Ackerman, T. Borch, L. Cary, S. Korf, Y. Odake, R. Schwend, and T. Stonoha for field and/or analytical work, as well as support from the Stanford Synchrotron Radiation Lightsource (SSRL) including technical assistance from S. Webb, S. Fendorf, J. Bargar, and T. Borch. Funding for this research was provided by the National Aeronautics and Space Administration (NASA) Exobiology Program (via funds provided to the Thermal Biology Institute, MSU), the NSF IGERT Program (0654336), and the Montana Agricultural Experiment Station (911300). Permitting for this work was facilitated by C. Hendrix and T. Olliff (Center for Resources, YNP; Permit YELL-2007-2008-SCI-5068).

REFERENCES

Ackerman GG(2006) Biogeochemical gradients and energetics in geothermal systems of Yellowstone National Park. M.S. Thesis. Montana State University. Bozeman, Montana, USA.

Allen ET, Day A (1935) *Hot Springs of the Yellowstone National Park*. Carnegie Institute of Washington Publications, Washington, DC, 466.

Allison JD, Brown DS, Novo-Gradac KJ(1991) *MINTEQ A2/PRODEFA2, a Geochemical Assessment Model for Environmental Systems: Version 3.0 User's Manual*. Environmental Research Laboratory, Office of Research and Development, USEPA, Athens, Georgia.

Amend JP, Shock EL (2001) Energetics of overall metabolic reactions of thermophilic and hyperthermophilic Archaea and Bacteria. *FEMS Microbiology Reviews* **25**, 175–243.

Amend JP, Rogers KL, Shock EL, Gurrieri S, Inguaggiato S (2003) Energetics of chemolithotrophy in the hydrothermal system of Volcano Island, southern Italy. *Geobiology* **1**, 37–58.

APHA (1998) Standard Methods for the Examination of Water and Wastewater(eds Clesceri AS , Greenberg AW, Eaton AD). American Public Health Association, Washington.

Ashelford KE, Chuzhanova NA, Fry JC, Jones AJ, Weightman AJ (2006) New screening software shows that most recent large 16S rRNA gene clone libraries contain chimeras. *Applied and Environmental Microbiology* **72**, 5734–5741.

Baker GC, Cowan DA (2004) 16S rDNA primers and the unbiased assessment of thermophile diversity. *Biochemical Society Transactions* **32**, 218–221.

Beam JP, Jay ZJ, Kozubal MA, Inskeep WP. (2011) Distribution and ecology of thaumarchaea in geothermal environments. The 11th International Conference on Thermophiles Research, September 11-16, Big Sky MT, Abstr. PA-009.

Berg IA, Ramos-Vera WH, Petri A, Huber H, Fuchs G (2010) Study of the distribution of autotrophic CO_2 fixation cycles in Crenarchaeota. *Microbiology* **156**, 256–269.

Blumentals II, Itoh M, Olson GJ, Kelly RM (1990) Role of polysulfides in reduction of elemental sulfur by the hyperthermophilic archaebacterium *Pyrococcus furiosus. Applied and Environmental Microbiology* **56**, 1255–1262.

Boulegue J (1978) Solubility of elemental sulfur in water at 298 K. *Phosphorus Sulfur* **5**, 127–128.

Boyd ES, Jackson RA, Encarnacion G, Zahn JA, Beard T, Leavitt WD, Pi Y, Zhang CL, Pearson A, Geesey GG. (2007) Isolation, characterization, and ecology of sulfur-respiring Crenarchaea inhabiting acid-sulfate-chloride-containing geothermal springs in Yellowstone National Park. *Applied and Environmental Microbiology* **73**, 6669–6677.

Brochier-Armanet C, Boussau B, Gribaldo S, Forterre P (2008) Mesophilic crenarchaeota: proposal for a third archaeal phylum, the Thaumarchaeota. *Nature Reviews* **6**, 245–252.

D'Imperio S, Lehr CR, Oduro H, Druschel G, Kuhl M, McDermott TR (2008) Relative importance of H_2 and H_2S as energy sources for primary production in geothermal springs. *Applied and Environmental Microbiology* **74**, 5802–5808.

Donald R, Southam G (1999) Low temperature anaerobic bacterial diagenesis of ferrous monosulfide to pyrite. *Geochimica et Cosmochimica Acta* **63**, 2019–2023.

Druschel GK, Baker BJ, Gihring TM, Banfield JF (2004) Acid mine drainage biogeochemistry at Iron Mountain, California. *Geochemical Transactions* **5**, 13–32.
Eder W, Huber R (2002) New isolates and physiological properties of the Aquificales and description of *Thermocrinis albus* sp. nov. *Extremophiles* **6**, 309–318.
Fillella M, May PM (2003) Computer simulation of the low-molecular-weight inorganic species distribution of antimony(III) and antimony(V) in natural waters. *Geochemica et Cosmochimica Acta*. **67**, 4013–4031.
Fischer F, Zillig W, Stetter KO, Schreiber G (1983) Chemolithoautotrophic metabolism of anaerobic extremely thermophilic archaebacteria. *Nature* **301**, 511–513.
Fournier RO(2005) Geochemistry and Dynamics of the Yellowstone National Park Hydrothermal System. In *Geothermal Biology and Geochemistry in Yellowstone National Park* (eds WP Inskeep, McDermott TR). Thermal Biology Institute, Montana State University, Bozeman, Montana, pp. 3–29.
Ghosh W, Dam B (2009) Biochemistry and molecular biology of lithotrophic sulfur oxidation by taxonomically and ecologically diverse bacteria and archaea. *FEMS Microbiology Reviews* **33**, 999–1043.
Gurial M, Tron P, Aubert C, Gloter A, Iobbi-Nivol C, Giudici-Orticoni M-T (2005) A membrane-bound hydrogen-oxidizing and sulfur reducing complex from the hyperthermophilic bacterium *Aquifex aeolicus*. *Journal of Biological Chemistry* **280**, 42004–42015.
Handley KM, Campbell KA, Mountain BW, Browne PRL (2005) Abiotic-biotic controls on the origin and development of spicular sinter: in situ experiments, Champagne Pool Waiotapu, New Zealand. *Geobiology* **3**, 93–114.
Helz GR, Tossell JA (2008) Thermodynamic model for arsenic speciation in sulfidic waters: a novel use of ab initio computations. *Geochimica et Cosmochimica Acta* **72**, 4457–4468.
Holloway JM, Nordstrom DK, Bohlke JK, McCleskey RB, Ball JW (2011) Ammonium in thermal waters of Yellowstone National Park: processes affecting speciation and isotope fractionation. *Geochimica et Cosmochimica* **75**, 4611–4636.
Huber H, Stetter KO(2006) Desulfurococcales In *The Prokaryotes* (eds Dworkin M, Falkow S, Rosenberg E, Schleifer K-H, Stackebrandt E) Springer, New York. pp. 52–68.
Huber G, Spinnler C, Gambacorta A, Stetter KO (1989) *Metallosphaera sedula* gen. and sp. nov. represents a new genus of aerobic, metal-mobilizing, thermoacidophilic archaebacteria. *Systematic and Applied Microbiology* **12**, 38–47.
Huber R, Eder W, Heldwein S, Wanner G, Huber H, Rachel R, Stetter KO (1998) *Thermocrinis ruber*, gen nov., sp. nov., a pink filament-forming hyperthermophilic bacterium isolated from Yellowstone National Park. *Applied and Environmental Microbiology* **64**, 3576–3583.
Huber R, Sacher M, Vollmann A, Huber H, Rose D (2000) Respiration of arsenate and selenate by hyperthermophilic archaea. *Systematic and Applied Microbiology*, **23**, 305–314.
Huber H, Huber R, Stetter KO(2006) Thermoproteales In *The Prokaryotes*(eds Dworkin M, Falkow S, Rosenberg E, Schleifer K-H, Stackebrandt E) Springer, New York. pp. 10–22.
Inskeep WP, Ackerman GG, Taylor WP, Kozubal MA, Korf S, Macur RE (2005) On the energetics of chemolithotrophy: case studies of geothermal springs in Yellowstone National Park. *Geobiology* **3**, 297–317.
Inskeep WP, Rusch DB, Jay ZJ, Herrgard MJ, Kozubal MA, Richardson TH, Macur RE, Hamamura N, Jennings RM, Fouke BW, Reysenbach A-L, Roberto F, Young M, Schwartz A, Boyd ES, Badger JH, Mathur EJ, Ortmann AC, Bateson M, Geesey G, Frazier M (2010) Metagenomes from high-temperature chemotrophic systems reveal geochemical controls on microbial community structure and function. PLoS ONE 5, e9773. doi:10.1371/journal.pone. 0009773
Itoh T, Suzuki K, Nakase T (1998) *Thermocladium modestius* gen. nov., sp. nov., a new genus of rod-shaped, extremely thermophilic crenarchaeote. *International Journal of Systematic Bacteriology* **48**, 879–887.
Itoh T, Suzuki K, Sanchez PC, Nakase T (1999) *Caldivirga maquilingensis* gen. nov., sp. nov., a new genus of rod-shpaed crenarchaeote isolated from a hot spring in the Philippines. *International Journal of Systematic Bacteriology* **49**, 1157–1163.
Itoh T, Suzuki K, Nakase T (2002) *Vulcanisaeta distributa* gen. nov., sp. nov., and *Vulcanisaeta souniana* sp. nov., novel hyperthermophilic, rod-shaped crenarchaeotes isolated from hot springs in Japan. *International Journal of Systematic and Evolutionary Microbiology* **52**, 1097–1104.
Itoh T, Nomura T, Sako Y (2003) Distribution of 16S rRNA introns among the family Thermoproteaceae and their evolutionary implications. *Extremophiles* **3**, 229–233.
Jahn U, Huber H, Eisenreich W, Hugler M, Fuchs L (2007) Insights into the autotrophic CO_2 fixation pathway of the Archaeon *Ignicoccus hospitalis*: comprehensive analysis of the central carbon metabolism. *Journal of Bacteriology* **189**, 4108–4119.
Jay ZJ, Planer-Friedrich B, Rusch DB, Inskeep WP (2011) Linking geochemistry to microbial community structure and function in sulfidic geothermal systems of Yellowstone National Park. Goldschmidt Conference, August 2011, Prague, CR. *Mineralogical Magazine* **75**, 1104.
Jorgensen BB (1990) A thiosulfate shunt in the sulfur cycle of marine sediments. *Science* **249**, 152–154.
Kashefi K, Holmes DE, Reysenbach A-L, Lovley DR (2002) The use of Fe(III) as an electron acceptor to recover preciously uncultured hyperthermophiles: isolation and characterization of *Geothermobacterium ferrireducens* gen nov., sp. nov. *Applied and Environmental Microbiology* **68**, 1735–1742.
Kletzin A, Urich T, Muller F, Bandeiras TM, Gomes CM (2004) Dissimilatory oxidation and reduction of elemental sulfur in thermophilic archaea. *Journal of Bioenergetics and Biomembranes* **36**, 77–91.
Laska S, Lottspeich F, Kletzin A (2003) Membrane-bound hydrogenase and sulfur reductase of the hyperthermophilic and acidophilic archaeon *Acidianus ambivalens*. *Microbiology* **149**, 2357–2371.
Macur RE, Langner HW, Kocar BD, Inskeep WP (2004) Linking geochemical processes with microbial community analysis: successional dynamics in an arsenic-rich, acid-sulfate-chloride geothermal spring. *Geobiology* **2**, 163–177.
McCleskey RB, Ball JW, Nordstrom DK, Holloway JM, Taylor HE(2005) Water-chemistry data for selected hot springs, geysers, and streams in Yellowstone National Park, Wyoming 2001-2002. United States Geological Survey Open File Report 2004-1316 Boulder, Colorado.
Meyer-Dombard DR, Shock EL, Amend JP (2005) Archeal and bacterial communities in geochemically diverse hot springs of Yellowstone National Park, USA. *Geobiology* **3**, 211–227.
Nomura N, Sako Y (1998) Molecular characterization and postsplicing fate of three introns within the single rRNA operon of the hyperthermophilic archaeon *Aeropyrum pernix* K1. *Journal of Bacteriology* **180**, 3635–3643.
Perevalova AA, Kolganova TV, Birkeland N-K, Schleper C, Bonch-Osmolovskaya EA, Lebedinsky AV (2008) Distribution

of Crenarchaeota representatives in terrestrial hot springs of Russia and Iceland. *Applied and Environmental Microbiology* **74**, 7620–7628.
Pfenning N, Lippert KD (1966) Über das vitamin B_{12}-bedürfnis phototropher schwefelbakterien. *Archives of Microbiology* **55**, 245–256.
Phoenix VR, Renaut RW, Jones B, Ferris FG (2005) Bacterial S-layer preservation and rare arsenic-antimony-sulphide bioimmobilization in siliceous sediments from Champagne Pool hot spring, Waiotapu, New Zealand. *Journal of the Geological Society* **162**, 323–331.
Planer-Friedrich B, London J, McCleskey RB, Nordstrom DK, Wallschlager D (2007) Thioarsenates in geothermal waters of Yellowstone National Park: determination, preservation and geochemical importance. *Environmental Science and Technology* **41**, 5245–5251.
Planer-Friedrich B, Fisher JC, Hollibaugh JT, Sub E, Wallschlager D (2009) Oxidative transformations of trithioarsenate along alkaline geothermal drainages- abiotic versus microbially mediated processes. *Geomicrobiology Journal* **26**, 339–350.
Prokofeva MI, Kublanov IV, Nercessian O, Tourova TP, Kolganova TV, Lebedinsky AV, Bonch-Osmolovskaya EA, Spring S, Jeanthon C (2005) Cultivated anaerobic acidophilic/acidotolerant thermophiles from terrestrial and deep-sea hydrothermal habitats. *Extremophiles* **9**, 437–448.
Ramos-Vera WH, Berg IA, Fuchs G (2009) Autotrophic carbon dioxide assimilation in Thermoproteales revisited. *Journal of Bacteriology* **191**, 4286–4297.
Rawlings DE (2002) Heavy metal mining using microbes. *Annual Reviews of Microbiology* **56**, 65–91.
Reysenbach AL, Shock EL (2002) Merging genomes with geochemistry at hydrothermal ecosystems. *Science* **296**, 1077–1082.
Rogers KL, Amend JP (2005) Archaeal diversity and geochemical energy yields in a geothermal well on Vulcano Island, Italy. *Geobiology* **3**, 319–332.
Rogers KL, Amend JP (2006) Energetics of potential heterotrophic metabolisms in the marine hydrothermal system of Vulcano Island, Italy. *Geochimica et Cosmochimica Acta* **70**, 6180–6200.
Segerer A, Neuner AM, Kristjansson JK, Stetter KO (1986) *Acidianus infernus* gen. nov., sp. nov., and Acidianus brierleyi comb. nov.: facultatively aerobic, extremely acidophilic thermophilic sulfur-metabolizing archaebacteria. *International Journal of Systematic Bacteriology* **36**, 559–564.
Spear JR, Walker JJ, McCollom TM, Pace NR (2005) Hydrogen and bioenergetics in the Yellowstone geothermal ecosystem. *Proceedings of the National Academy of Sciences of United States of America* **102**, 2555–2560.
Tamura K, Dudley J, Nei M, Kumar S (2007) MEGA4: Molecular Evolutionary Genetics Analysis (MEGA) software version 4.0. *Molecular Biology and Evolution* **24**, 1596–1599.
Vairavamurthy A, Manowitz B, Luther GW, Jeon Y (1993) Oxidation state of sulfur in thiosulfate and implications for anaerobic energy metabolism. *Geochimica et Cosmochimica Acta* **57**, 1619–1623.
Volkl P, Huber R, Drobner E, Rachel R, Burggraf S, Trincone A, Stetter KO (1993) *Pyrobaculum aerophilum* sp. nov., a novel nitrate-reducing hyperthermophilic archaeum. *Applied and Environmental Microbiology* **59**, 2918–2926.
Webb SM (2005) SIXpack: a graphical user interface for XAS analysis using IFEFFIT. *Physica Scripta* **115**, 1011–1014.
Wolin EA, Wolin MJ, Wolfe RS (1963) Formation of methane by bacteria extracts. *The Journal of Biological Chemistry* **238**, 28–34.
Xu Y, Schoonen MAA, Nordstrom DK, Cunningham KM, Ball JW (1998) Sulfur geochemistry of hydrothermal waters in Yellowstone National Park: I The origin of thiosulfate in hot spring waters. *Geochimica et Cosmochimica Acta* **62**, 3729–3743.
Xu Y, Schoonen MAA, Nordstrom DK, Cunningham KM, Ball JW (2000) Sulfur geochemistry of hydrothermal waters in Yellowstone National Park, Wyoming, USA II. Formation and decomposition of thiosulfate and polythionate in cinder pool. *Journal of Volcanology and Geothermal Research* **97**, 407–423.
Zillig W, Stetter KO, Prangishvilli D, Schafer W, Wunderl S, Janekovic D, Holz I, Palm P (1983) Desulfurococcaceae, the second family of the extremely thermophilic, anaerobic, sulfur-respiring Thermoproteales. *Zentralbl Bakteriol Parasitenkd Infektionskr Hyg Abt* **3**, 304–317.

SUPPORTING INFORMATION

Additional Supporting Information may be found in the online version of this article:

Figure S1. Synchrotron X-ray diffraction patterns of samples collected from Joseph's Coat, Monarch Geyser, and Cistern Spring (Yellowstone National Park). JC3A bottom is composed primarily of quartz (PDF#46-1045), while JC3A sediment is composed primarily of quartz (PDF#46-1045), pyrite (PDF#42-1340), and stibnite (PDF#42-1393). Monarch Geyser and Cistern Spring both contain distinct patterns representative of elemental sulfur (PDF#08-0247 and PDF#89-2600, respectively).

Figure S2. Linear combination antimony EXAFS fitting of solid phases present in samples collected from Joseph's Coat Hot Spring (Yellowstone National Park). All samples exhibit a large contribution from stibnite (Sb_2S_3), with most remaining variation explained by contributions from Sb (V) [JC3A south and northwest samples represent the stibnitic metallic phase vs. the cooler JC3A sediment]. Least-squares fitting confirmed that Sb(III) standards other than stibnite (e.g., Na antimonite, Sb_2O_3) represented less than 10% mole fraction of antimony in all samples (^{1} reduced chi-square parameter to indicate goodness of fit).

Table S1. Average source water chemistry (total dissolved concentration) of three sulfidic geothermal springs located at Joseph's Coat Springs (JC3) and Norris Geyser Basin (NGB), Yellowstone National Park (standard deviations in parentheses).

Table S2. Exergonic (i.e., thermodynamically-favorable) oxidation-reduction reactions involving aqueous and solid phase species important in geothermal environments of Joseph's Coat Spring, Monarch Geyser and Cistern Spring. Reactions highlighted in gray involve sulfur species. The free energy values (ΔG_{rxn}, kJ mol^{-1} e^{-1}) for each reaction are given at 85 °C (ΔG_{rxn} calculated using activities of chemical species predicted using aqueous chemical modeling, MINTEQ).

Table S3. Saturation indices [log (IAP/K_{SP})] with respect to various mineral phases calculated after chemical speciation with the aqueous equilibrium program, Visual MINTEQ (IAP = ion activity product; Ksp = solubility product constant; SI > 0 = over-saturation; SI < 0 = under-saturation).

Table S4. Evaluation of potential carbon and energy sources and possible electron acceptors supporting growth of *Pyrobaculum*-like strain WP30. Experiments were conducted in 100% synthetic medium contained in 10 mL serum bottles at 75 °C and pH 6.1 [entries highlighted in gray supported significant growth and/or production of sulfide; nd = not detectable; YE = yeast extract].